In Vitro Degradation of Starch/PVA Films and Biocompatibility Evaluation

Rui Shi,[1] Aichen Zhu,[2] Dafu Chen,[1] Xiujuan Jiang,[2] Xiaochuan Xu,[3] Liqun Zhang,[1] Wei Tian[2,3]

[1]*Laboratory of Bone Tissue Engineering of Beijing Research Institute of Traumatology and Orthopaedics, Beijing 100035, People's Republic of China*
[2]*The Key Laboratory of Beijing City on Preparation and Processing of Novel Polymer Materials, Beijing University of Chemical Technology, Beijing 100029, People's Republic of China*
[3]*Beijing JiShuiTan Hospital, Fourth Clinical Medical College of Peking University, Beijing 100035, People's Republic of China*

Received 15 December 2008; accepted 15 July 2009
DOI 10.1002/app.31136
Published online 27 August 2009 in Wiley InterScience (www.interscience.wiley.com).

ABSTRACT: A series of starch/PVA (SP) films with the thickness of 0.05–0.1 mm were cast by solvent method. The swelling and degradation behaviors in simulated blood fluid (SBF) and simulated saliva fluid (SSF) within 30 days were investigated. *In vitro* biocompatibility was also evaluated. Research purpose of this work was to supply basic data for SP films' potential application in guide tissue regeneration (GTR) technology. It took 10–20 min for different samples to reach to their maximum water absorption and 30 min to lever off. The weight loss of all samples decreased rapidly in the first day in both of SBF or SSF, and then it changed slightly in SSF but decreased step by step in SBF. The mechanical properties of the wet SP films were satisfied with the requirement of GTR membrane. No matter in SBF or SSF, although the mechanical properties decreased rapidly in the first day, they changed slightly after that. Cytotoxicity and L929 fibroblasts attachment test proved that the SP film possesses excellent cell affinity. Hemolysis ratios of all samples were less than 5%. All results demonstrated that SP film is a promising candidate in GTR treatment. © 2009 Wiley Periodicals, Inc. J Appl Polym Sci 115: 346–357, 2010

Key words: degradation; swelling; biocompatibility

INTRODUCTION

In recent years, tissue engineering has been regarded as an ultimate medical treatment for reconstruction of defective tissues in biomedical engineering fields.[1] Guided tissue regeneration (GTR) is a comparatively simple tissue engineering treatment that reconstructs new tissue by using a barrier membrane to guard the defected area from invasion of other tissues. Recently GTR treatment and relevant biomaterials have been paid special attention by many researchers.[2–6] In the market of GRT membranes, conventional materials mainly include nondegradable, expanded polytetrafluoroethylene (ePTFE: Gore-Texs)[7–9] and degradable polylactic acid (Guidors).[10–13] Although e-PTFE membranes have achieved excellent clinical results, second surgery procedure is required to remove the membranes after new bone's generation. Otherwise, degradable GTR membranes have a benefit to avoid secondary surgery, and this will lighten the burden of patients. However, there are still a lot of problems with the existing biodegradable GTR membranes. GTR membranes are composed of polylactic acid (PLA), lactide polymers (PLGA) and their blending or copolymers will produce different acid products during their degradation and resorption process. The accumulation of acid products will significantly reduce the pH value, which will result in inflammatory response.[14,15] Collagen membrane had excellent cell affinity and biocompatibility to regenerate tissues. However, membrane made from collagen is normally weak in strength, and is therefore difficult to manipulate. Furthermore, the resorption rate is difficult to match with normal tissue-healing process. Therefore, GTR membranes with excellent mechanical properties, suitable degradation speed and good biocompatibility are required. The aim of this research is to find a kind of more suitable biomaterial to satisfy the requirements of GTR technology.

The composites of synthetic and natural biodegradable polymers have received growing interest due to their potential applications in biomedical field. By this way, the good mechanical properties and process ability of synthetic polymers can be combined with the specific tissue and cell compatibility of biopolymers.[16]

Correspondence to: L. Zhang (zhanglq@mail.buct.edu.cn) and W. Tian (tianweia@163bj.com).

Contract grant sponsor: Beijing Natural Science Foundation; contract grant number: 2061002.
Contract grant sponsor: Beijing Municipal Science and Technology Commission; contract grant number: Z080003032208013.

Polysaccharides, such as starch and dextran, are typical examples of natural biodegradable hydrophilic polymers with relatively good biocompatibility. Starch-based polymers and composites have been introduced as promising biomaterials for orthopaedic applications.[17–21] However, as polysaccharides dissolve easily in water, they do not have the mechanical and shape stability in body fluid. An effective method is to blend them with a synthesized polymer gel networks to form natural and synthesized polymer blend hydrogels. Among the existing synthesized polymers, PVA possesses many useful properties (biodegradable, nontoxic, and noncarcinogenic) that make it excellent biomaterial for biomedical application,[22] such as contact lenses,[23] artificial heart valves,[24,25] and drug delivery carriers,[26,27] cartilage,[28,29] and artificial pancreas.[30] To combine sufficient mechanical strength and flexibility of PVA with the excellent biocompatibility of the starch, we are interested in developing starch/PVA GTR membranes.

Although the mechanical properties and biodegradability of the SP films have already been researched by several researchers,[31–33] all of these studies were focused on the application in environment field so that the degradation always carried on in the medium like soil, water and bacteria, etc. According to our knowledge, there was no report related to the application of SP films in GTR technology which needs proper biodegradation rate and excellent biocompatibility.

It was reported that the regeneration capacity of the periodontal cells was the most strongest after 1 to 2 weeks' surgery, and decreased after 3 weeks. So it was considered that the GTR membrane should keep its integrity and mechanical properties for at least 3–4 weeks.[34,35] The *in vitro* degradation is the first and very important step for the GTR application purpose evaluation. Therefore, we investigated the degradation behaviors of the SP films both in SBF and SSF within 30 days.

Besides the biodegradability, the biocompatibility is also crucial for implant materials. As the blood contact material, the SP films were characterized by the hemolysis analysis. Cytotoxicity test and cell attachment observation were utilized to learn the cell-compatibility of the SP films.

In this study, the mechanical property, degradation performance and biocompatibility of the SP films were investigated. The aim of this study is to enrich the biomaterial categories of GTR membrane, search for the new application area of the starch/PVA composites, and supply basic data for the clinical application of SP films in GTR technology and other tissue repairing field, such as periodontal defects repairing, bone defect covering and bone substitutes, skin wound repairing and healing, as well as antibiotic and growth factors carrier, etc.

EXPERIMENTAL

Materials and preparation

The corn starch was supplied by J&k Co. (Japan), which was composed of 25% amylose and 75% amylopectin. The original moisture content was around 12%. The glycerol (AR) was obtained from Century Star Chemical Products Inc. (Beijing, China). PVA was obtained from Shanghai Reagent Company (Shanghai, China), which was 99% hydrolyzed with an average polymerization degree of 1750 ± 50. The water used to prepare starch/PVA blend films was redistilled after deionization.

Films were obtained by the casting method. First, the solution was prepared by dissolving PVA, starch and glycerol in hot water. The mixture was blended for 5 h with a mechanical stirrer (1000 rpm) at 95°C to form a homogeneously gel-like solution. Bubbles were removed with an aspirator. The ratio of PVA to starch (w : w) were 4 : 1, 3 : 1, 2 : 1, and 1 : 1, named P4S1, P3S1, P2S1 and P1S1 respectively. The glycerol took up 20 wt % of the dry weight, and water takes up 13%. The certain amount of gel-like solution thus prepared was poured on a glass plate. Water was evaporated from the molds at 25°C for 15 h, The dried films were sealed in polyethylene bags and stored at 20°C and at 50% RH for 1 week before performing the measurements.

Composing of SBF and SSF

The ion concentrations of simulated body fluid (SBF) are nearly equal to those of the human body blood plasma, as shown in Table I.[36] The SBF solution was buffered at pH 7.4 with trimethanol aminomethane-HCl.

The composing of the simulated saliva fluid (SSF) was showed in Table II,[37] the pH was adjusted to 7.2 using KOH. Methyl-*p*-hydroxybenzoate serves as a preservative, while sodium carboxymethyl cellulose increased the viscosity of the artificial saliva to mimic the viscous natural saliva. The other constituents provided the inorganic components necessary for the remineralisation process at levels comparable to that of natural saliva. The concentration of α-amylase of healthy people is 0.04–0.4 g/L, but it is distinguished from different people and periods in one day. Considering the destruction during storage and the experimental course, we chose the concentration as 0.6 g/L which was little higher than that in normal human's saliva.[38] The α-amylase used was Type 11-A, SDS-PAGE (Sigma) with the molecular weight of 50–55 kDa. The active unit is 1500–3000 U/mg.

In vitro degradation in SBF and SSF

The samples for weight loss and swelling degree (SD) test were squared with about 0.05–0.1 mm

TABLE I
Ion Concentration of SBF in Comparison with Human Blood Plasma

	Concentration (m*M*)							
	Na^+	K^+	Ca^{2+}	Mg^{2+}	HCO_3^-	Cl^-	H_4^{2-}	SO_4^{2-}
SBF	142.0	5.0	2.5	1.5	4.2	148.5	1.0	0.5
Blood plasma	142.0	5.0	2.5	1.5	27.0	103.0	1.0	0.5

thickness and 2 cm length of side. The degradation samples for tensile test were Dumb-bell shaped with 0.05–0.1 mm thickness and 4 mm width. The samples for tear test were 0.05–0.1 mm thickness. The samples were immersed in SBF or SSF which content in small vials. Then the vials were incubated in a shaking incubator at 100 rpm at 37°C for 4 weeks. The SBF was refreshed every week, and the SSF was refreshed every day.

Characterization

Weight loss

The weight loss was calculated by comparing the dry weight (W_d) of the remained sample after degradation for a predetermined time with the original dry weight (W_0) of the sample as the eq. (1). At predetermined intervals of 0, 3, 7, 14, and 30 d; samples were taken out, purged with distilled water and subsequently dried until absolute desiccation, then weighted.

$$\text{Weight loss } (\%) = \frac{W_0 - W_d}{W_0} \times 100 \qquad (1)$$

Swelling degree (SD)

The SD was characterized at 37°C. The experiments were carried out by measuring the weight gain as a function of immersion time in 20 mL solution. The SD was calculated according to eq. (2)

$$\text{Swelling degree } (\%) = \frac{W_t - W_o}{W_o} \times 100 \qquad (2)$$

Where W_t is the wet weight and after degrading a predetermined time, W_o is the original weight of the sample.

Contact angle (CA) measurement

Static contact angle (CA) of distilled water on the smooth polymer surface were used to evaluate the hydrophilicity, which was measured by a CA meter (OCA-20, Germany). Angles were measured on five different regions of each polymer sample at 25°C and the result averaged.

Mechanical measurement

The mechanical properties of polymer films were measured on an EXL750/EZ 01/2914 LLOYD (England) tester at a crosshead speed of 10 mm/min at room temperature. Tear strength was carried out according to ISO 34–1 1994. Five samples were tested and the average of the values was taken.

Differential scanning calorimeter (DSC)

DSC thermograms were recorded by a NETZSCH DSC 204 F1 (Germany) instrument. The sample (3–10 mg) placed in aluminium pan was firstly cooled from room temperature to −120°C and hold there for 3 min. Subsequently, a heating scan was conducted from −120 to 150°C at a heating rate of 20°C/min. The glass transition temperature was taken as the midpoint of the heat capacity change.

Morphological studies by scanning electron microscopy (SEM)

The surface morphology of the SP films before and during degradation was observed in Hitachi S-4700 scanning electron microscope. The samples were previously sputter-coated with gold. Microphotographs were taken at various magnifications.

Cytotoxicity test

The samples were incubated in phosphate buffered saline (PBS) solution for 8 h to decrease the effects of the impurity on cells. The 0.1 mm thickness slices were sterilized by washing with a 75% (v/v) ethanol solution in sterilized water, followed by CO_{60} exposure for 15 min, and then incubated in Dulbecco's modified Eagle's medium (DMEM) with the proportion of 3 cm^2/mL for 24 h at 37°C. The extract solution was then filtrated (0.22 μm pore size) to eliminate the possible presence of solid particles of the

TABLE II
The Concentration of the Components in SSF

Components	Concentrations
Methyl-*p*-hydroxybenzoate	2.00 g/L
Sodium carboxymethyl cellulose	10.0 g/L
KCl	8.38 m*M*
$MgCl_2.6H_2O$	0.29 m*M*
$CaCl_2{\cdot}2H_2O$	1.13 m*M*
K_2HPO_4	4.62 m*M*
KH_2PO_4	2.40 m*M*
Fluoride	0.022 ppm
α-amylase	0.60 g/L

material. L929 cells were cultured in DMEM supplemented with 10% (v/v) fetal bovine serum (FBS) at a density of 4.0×10^4 cells/mL and plated into 96-well micrometer plates. The plates were incubated for 24 h at 37°C in a humidified atmosphere with 5% CO_2 in air. After that, the medium was replaced by the previous prepared extracted dilutions (50%, volume proportion), using culture medium by itself as a control. After 2, 4, 7 day's incubation, the cell culture was treated with MTT test. 50 mL/well of MTT (1 mg/mL in medium 199 without phenol red, Sigma, St. Louis) and incubated for further 4 h at 37°C in a humidified atmosphere of 5% of CO_2 in air. At this stage the MTT was removed and 100 ml/well of isopropanol (BDH, Poole, England) was added to dissolve the formazan crystals. The optical density (OD) was read on a multiwell microplate reader (EL 312e Biokinetics reader, Biotek Instruments) at 570 nm. All materials extracts were tested for a minimum of three separate experiments with comparable results.

L929 cell culture

To investigate cell attachment and proliferation on SP films, cell culture studies were carried out with L929 mouse fibroblasts. The cells were subcultured in flasks using DMEM supplemented with 10% (v/v) FBS, and maintained at 37°C in a humidified CO_2 (5%) atmosphere. Cells were dissociated with 0.01% trypsin/10 m*M* EDTA, centrifuged and resuspended in medium. The culture medium was replaced every 2 day. Before cell culture experiments, 24-well tissue culture plates were precoated with parafilm, then soaked in 96% ethanol and placed under UV light for 30 min for sterilization. SP films with 13 mm diameter were sterilized with 70% ethanol (15 min, 2 times), rinsed with sterile Dulbecco's PBS (pH 7.4, 30 min, 2 times) and suspended in conditioning medium (15 min). For cell attachment experiments, the cell density was adjusted to 5×10^4 cells/mL in DMEM containing 10% FBS. One milliliter of cell suspension was added to each well of the 24-well TCPS containing SP membranes. The adhesion, spreading and proliferation characteristics of the cells were observed by SEM.

Hemolysis ratio

The samples were cut into small pieces and the samples were equilibrated in normal saline water for 30 min at room temperature. Weight of each film was taken after drying it in air after which Wistar rats blood (0.2 mL) was added to each sample. After a predetermined time period, 4 ml of saline water added to each sample to stop hemolysis and those samples were kept at constant temperature (35°C) for 1 h. Positive and negative controls were produced by adding 0.2 mL of rat's blood to 4 ml of distilled water and saline water respectively. All the samples were centrifuged. OD of the supernatant was measured at 545 nm. The experiments were run in triplicate and were repeated twice. The percent of hemolysis was calculated as eq. (3):

$$\% \text{ Hemolysis} = \frac{\text{OD of test sample} - \text{OD } (-) \text{ control}}{\text{OD } (+) \text{ control} - \text{OD } (-) \text{ control}} \times 100 \quad (3)$$

RESULTS AND DISCUSSION

Swelling behaviors

Static water CA changes in the course of swelling

When the water dropped on surface of the film, the water contacted area swelled at once. Therefore, the CA increased in the process of swelling. The CA values of different SP films within 30 s were shown in Table III. The CA of all samples increased as the time increased within 30 s. We learned that the obvious swelling took place and the swelling rate was very fast in the first 30 s from the data listed in Table III. We also observed that when the swelling reached to a certain degree, the CA decreased as the time increased due to the strong water absorbability of the SP films. It took about 2 min for the water drips absorbing by the SP films, and the CA gradually tuned to 0°.

The CA is related with the swelling. It increased in the course of swelling (Fig. 1). Except P1S1, the CA decreased as the starch content increased at the same time intervals (Table III). It can be explained by that the density of hydroxyl groups on starch molecular was larger than that on PVA molecular, so the hydrophilicity of starch was better than that of PVA, and the swelling velocity increased as the starch content increased. The explanation for why the CA of P1S1 was larger than that of any other samples may be that the surface of the P1S1 was rougher than that of any other's [Fig. 5(b)]. Because there were more starch molecules in P1S1 than those in other samples, so it will be easier for the starch molecules reconnected

TABLE III
CA of Different SP Films as the Time Increased Within 30 s

Samples	CA/°						
	0 s	5 s	10 s	15 s	20 s	25 s	30 s
P4S1	53.5	57.5	59.3	66.0	68.8	76.8	82.9
P3S1	51.4	54.5	55.6	57.5	58.8	60.6	62.5
P2S1	32.4	35.7	38.8	39.3	42.4	45.3	47.8
P1S1	69.3	70.7	71.7	72.3	73.9	73.6	75.0

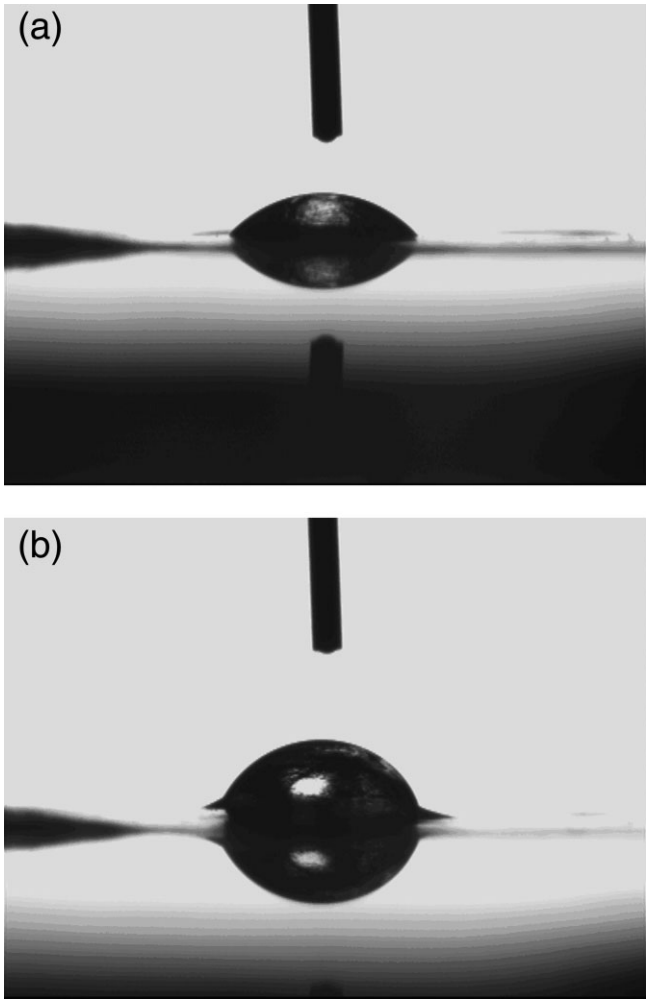

Figure 1 Images of the water drips dropped on surface of P1S1 immediately (a) and after 30 s (b).

together by hydrogen bonds. Therefore, the recrystallization of starch will take place easily in P1S1 than in any other samples. The recrystallization would result in the formation of the starch granules and relatively high surface roughness.[39]

Short time swelling behavior in water

Figure 2 shows the water absorption changing tendency of different SP films within 4 h. The water absorption increased as the starch percentage increased. That is because there are more hydroxyl

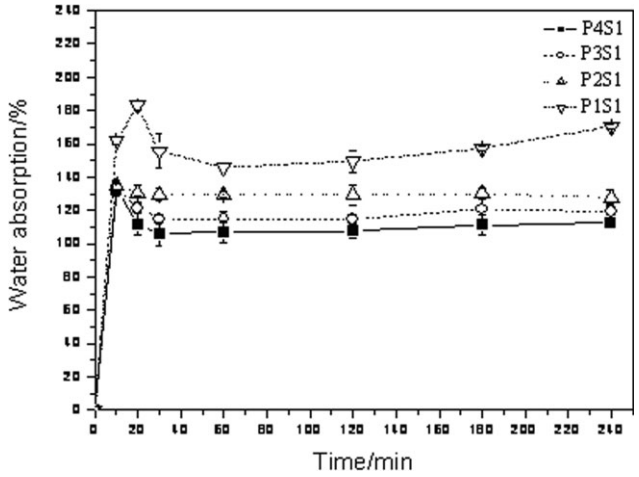

Figure 2 Time dependent water absorption (%) of different SP films within 4 h.

groups on starch molecules than those on PVA molecules. For the samples with different starch content, the water absorption increased quickly at the first 10 min. It took 10–20 min for different samples to reach to the maximum value. After that, the water absorption of all samples exhibited a little decrease. The water absorption variation trend was mainly affected by the hydrophilicity of the components and the glycerol liberation speed. At the first 10 min, because there are tremendous hydroxyl groups on the starch and PVA molecular, the water molecules quickly get into inter- and intra- macromolecules of starch and PVA. The water absorption speed was larger than the glycerol liberation speed at this stage.

When the starch and PVA molecules combined with sufficient water, the water absorption gradually became saturated and the absorption velocity was slowed down. When the water absorption speed is smaller than glycerol liberation speed, the SD exhibited a little decrease. When most of the glycerol dissolved into the water, a temporary equilibrium state exhibited.

Swelling behavior in SBF and SSF

The results of SD in SBF and SSF were showed in Table IV. For the samples with the same PVA/starch ratio, the SD in SBF was larger than that in SSF. This

TABLE IV
Time Dependent Swelling Degree (%) of the SP Films in SBF and SSF Within 30 Days

	Swelling degree/%									
	SBF					SSF				
Samples	1d	3d	8d	14d	30d	1d	3d	8d	14d	30d
P4S1	61.3	90.2	124.6	120.8	116.9	45.6	80.0	82.2	80.3	80.1
P3S1	72.2	95.6	119.9	113.7	110.0	44.5	74.9	75.6	73.8	72.1
P2S1	77.1	98.6	114.6	108.1	105.8	43.4	64.5	66.7	65.4	63.3
P1S1	78.8	102.4	109.5	106.8	103.1	37.6	47.8	48.1	47.6	46.2

phenomenon can be explained by that the α-amylase in SSF resulted in the very quick degradation of the starch.[40] Furthermore, the SD is also influenced by the solution viscosity. Because the viscosity of SSF is larger than that of the SBF, the SD and swelling speed in SSF should be smaller than that in SBF.

In SSF, the starch nearly got a completely degradation within 1 day,[40] so after the first day, the SD was mainly depended on the initial PVA content. The SD increased as the initial PVA content increased from the 1 to 30 d.

In SBF, a different swelling behavior was exhibited. We noticed that the SD increased as the starch percentage increased at the first 8 days. Because there is no amylase in SBF, the swelling behavior was coeffected by starch and PVA. Because the hydroxyl group density of starch molecule is larger than that of PVA molecule, the water-absorbing capacity increased as the starch content increased, and the SD increased as the initial starch content increased in the first 8 days. After this stage, with the gradually degradation of the starch, the SD was mainly influenced by the residual PVA. So after 8 days, the SD increased as the PVA percentage increased at the same observation intervals.

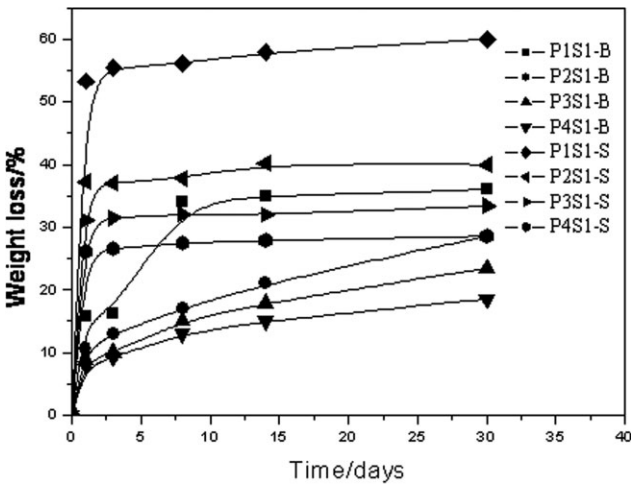

Figure 3 Time dependent weight loss (%) of the SP films in SBF and SSF within 30 days.

Degradation behavior in SBF and SSF within 30 days

Weight loss during degradation

The weight losses of different SP films in SBF and SSF on the 1st, 3rd, 8th, 14th, and 30th day were shown in Figure 3. "B" represents degradation in SBF and "S" represents degradation in SSF. Figure 3 reflects the regularity that for the samples with same starch content, the weight loss speed in SSF was much quicker than that in SBF, and the weight loss velocity increased as the starch content increased no matter in SBF or SSF.

In SSF, The weight losses of all samples exceeded the total weight percentage of starch and glycerol after 1 day's degradation. After that, the weight loss velocity went down. The results can be explained by that the starch in the composite quickly broke down into the short molecules, maltose and glucose on the first day. These degradation products quickly dissolved into the degradation liquid, so the residual composing was mainly PVA. From 1 day to 30 day, the decrease of the weight loss was very slightly. This phenomenon demonstrated that the degradation and dissolution rate of PVA was very slow in SSF under the normal body temperature.

In SBF, the weight loss velocity was very quick in the first day, and then exhibited a step by step increase manner. The quick weight loss on the first day was caused by the glycerol liberation. It has been demonstrated that the glycerol always dissolved into the water in the first few hours.[40] Because there are no amylase in the SBF, the starch molecular degraded more slowly in SBF than that in SSF.[40] The weight loss after the first day was mainly caused by the gradually breaking down of the starch molecules.

Changes of the mechanical properties during degradation

(1) Comparison of the mechanical properties of SP films in dry and wet state.

The GTR membranes were always applied in its wet state by dipping them in distilled water or physiological saline water before operation, so the mechanical properties of the wet films were very important. Before the mechanical testing, the films were dipped into the deionized water for 5 min. Then the samples were taken out immediately and the water on surface of the samples was absorbed by filter paper. The results were shown in Table V.

The tensile, tear strength and elongation at break (EB) of the SP films decreased quickly after dipping of the samples into the deionized water for 5 min (See Table V).

The values of the tensile strength, tear strength and elongation at break decreased as the starch content increased. Both the dry and wet film has the same regularity.

Although the mechanical properties decreased a lot in wet state compared to those in dry state, the wet SP films also kept the satisfied strength and flexibility. Even there are 50 wt % starch contained in the mixture, the tensile strength of P1S1 reached 1 MPa in the

TABLE V
Comparison of the Mechanical Properties of SP Films in Dry and Wet State

Samples	Tensile strength/ MPa		Tear strength/ MPa		Elongation at break/%	
	Dry	Wet	Dry	Wet	Dry	Wet
P4S1	34.6	3.9	128.8	27.7	213	166.3
P3S1	26.8	3.6	117.1	10.8	195	123.0
P2S1	22.3	2.9	98.8	8.3	168	121.6
P1S1	21.9	1.0	92.1	5.7	146	84.9

wet state. With respect to the requirement of GTR membranes, Ueyama et al.[41] reported that their calcium alginate GTR membranes had the tensile strength value of 0.017 MPa, which is satisfied with the GTR requirement. Compared to their result, it is considered that the tensile strength of SP membranes may be sufficient enough. Additionally, it must be mentioned that mechanical property of the SP films can be easily adjusted by varying the composition of the starch and PVA.

(2) Mechanical property changes during degradation.

As shown in Figure 4, no matter in SBF or SSF, the tensile strength, tear strength and elongation at break decreased quickly in the first day for all samples. However, the mechanical properties decreased little from 1 to 30 days.

At the degradation interval, the values of the mechanical property of the same sample were larger in SBF than those in SSF.

From the results of the tensile and tear testing, we noticed that for all samples, no matter in SBF or SSF, except a rapid decrease in the first day, the mechanical properties decreased slightly from 1 to 30 days, and the results demonstrates that the SP films possess good mechanical stability. Furthermore, the improvement of the mechanical properties can be achieved by increasing the PVA content in the mixture. The adjustable mechanical properties and the excellent mechanical maintainability in SBF and SSF are benefit for the SP films to be applied in different body positions, for example, periodontal defects, bone defect and skin wound repairing.

Morphology changes during degradation

P4S1 (a) and P1S1 (b) before degradation; P4S1 (c) and P1S1 (d) after 8 days' degradation in SBF; P4S1 (e) and P1S1 (f) after 8 days' degradation in SSF; P4S1 (g) and P1S1 (h) after 30 day's degradation in SBF; P4S1 (i) and P1S1 (j) after 30 day's degradation in SSF

The surface morphologies of P4S1 and P1S1 before degradation were shown in Figure 5(a,b). P4S1 has a homogeneous and smooth surface. A small number of white points are insoluble starch granules. The cracks were formed in the process of removing the brittle films from the mould. A large number of granules were observed on surface of the P1S1, which resulted in the surface roughness, and the

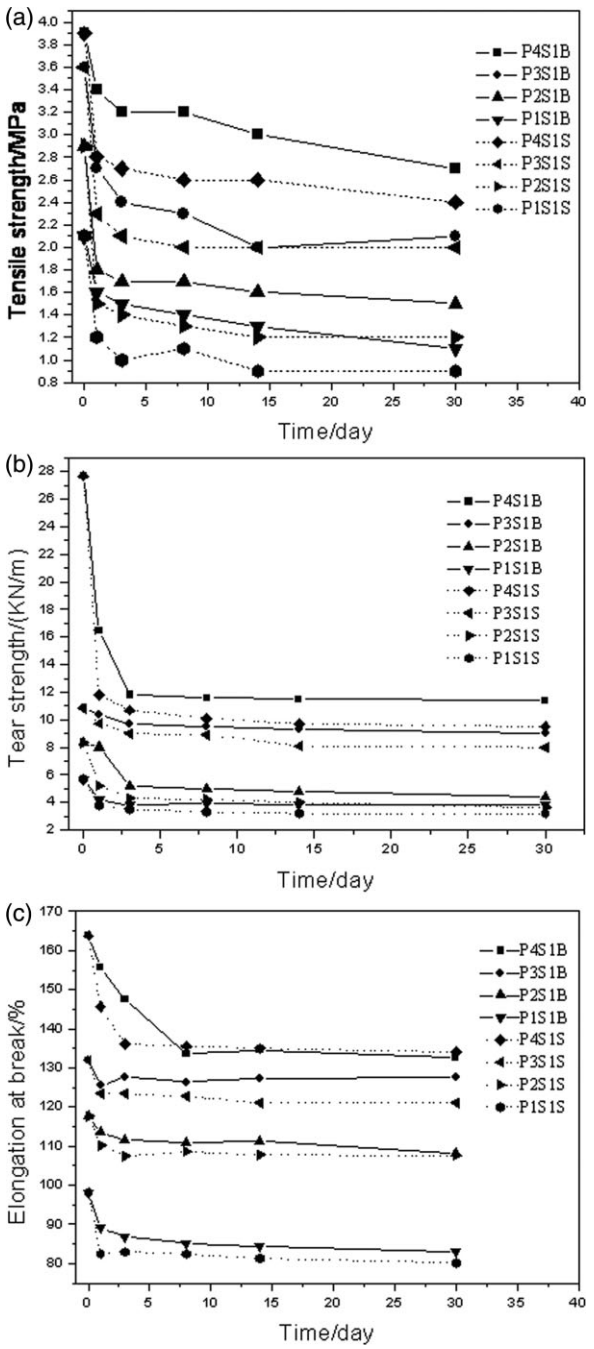

Figure 4 Tensile strength (a), tear strength (b) and elongation at break (c) of different samples with the time increased within 30 days.

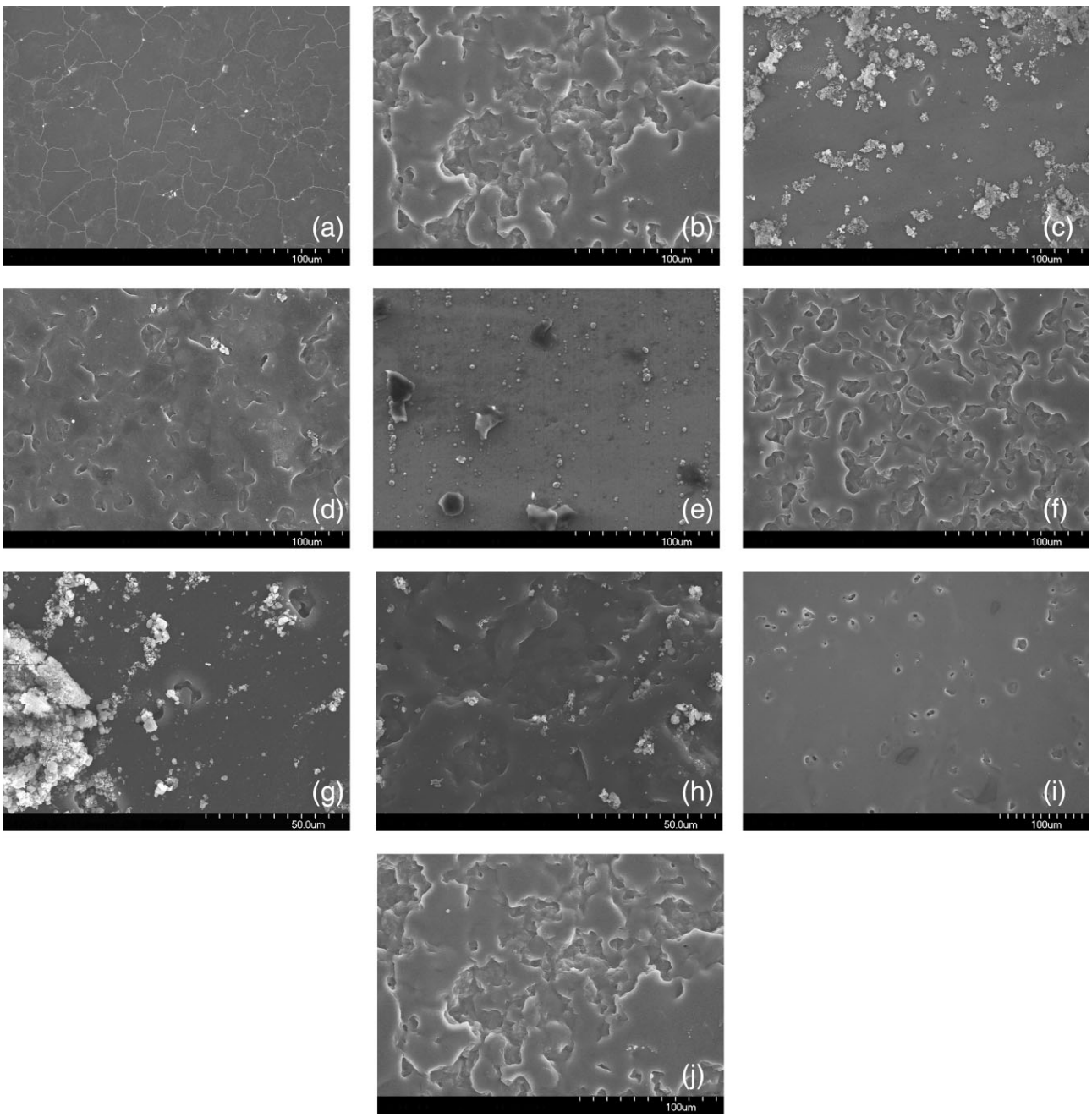

Figure 5 SEM micrographs of SP films in SBF and SSF during degradation P4S1 (a) and P1S1 (b) before degradation; P4S1 (c) and P1S1 (d) after 8 days' degradation in SBF; P4S1 (e) and P1S1 (f) after 8 days' degradation in SSF; P4S1 (g) and P1S1 (h) after 30 day's degradation in SBF; P4S1 (i) and P1S1 (j) after 30 day's degradation in SSF.

roughness could be caused by the phase separation in the process of molding.[42] Because there are more starch molecules in P1S1 than those in P4S1, the reconnection and rearrangement of the starch molecules took place much easier in P1S1 than those in P4S1, and that would result in the recrystallization and phase separation.

The surface morphology of the P4S1 and P1S1 after 8 days' degradation in SBF was shown in Figure 5(c,d). The white particles on surface were caused by the crystallization of the inorganic salts in degradation liquids. After 8 days' degradation, there were just a few of hollows on surface of the P4S1 [Fig. 5(c)]. However, a large number of hollows were observed on surface of the P1S1, and this phenomenon illustrated that the degradation speed increased as the starch content increased.

Comparing the surfaces of P4S1 with that of P1S1 after degraded in SSF for 8 days [see Fig. 5(e,f)], we can see obviously that there were more and bigger hollows on surface of the P1S1 than those on P4S1, and this phenomenon demonstrated that the

enzymatic decomposition speed of starch was also much larger than that of PVA. The α-amylase in SSF gave rise to the quick decomposition of the long starch molecules to short ones, maltose and glucose. The hollows were formed in the process of degradation products diffused into the degradation liquid.[40] Comprising the surfaces of P1S1 after 8 day's degradation in SSF and SBF respectively [Fig. 5(d,f)], we also learned that the degradation in SSF was much faster than that in SBF.

Surface morphologies of the samples after 30 days' degradation were shown in Figure 5(g–j). Figure 5 g and h exhibit the surfaces of P4S1 and P1S1 after degradation in SBF. Figure 5(i,j) show the surfaces of P4S1 and P1S1 after degradation in SSF.

From the SEM result after 30 days degradation, we learned that for the samples in same degradation liquid and after the same degradation time, the samples with more starch content degraded faster than those with less starch content. For the samples with the same starch/PVA ratio, the degradation in SSF was much faster than that in SBF.

It must be noticed that although some hollows were exhibited on surface of the SP films, the films could still keep their integrity even when the starch content reached to 50 wt % and buried in SSF for 30 days. The better integrity was observed when more PVA contained in the samples. The integrity maintainability within 30 days is also very important for the SP films to be used in GTR technology.

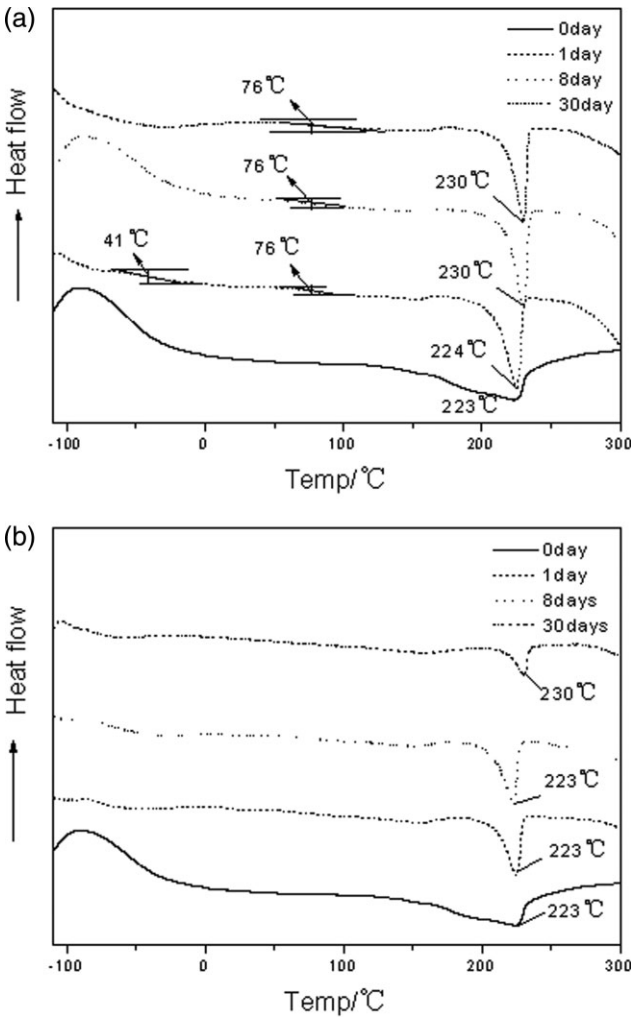

Figure 6 DSC curves of P1S1 before and after 1, 8, 30 days' degradation in SSF (a) and SBF (b).

DSC curve changes during degradation

Figure 6 depicts the DSC curve changes during degradation in SSF and SBF. Independently of the starch content, all the samples showed the two thermal transitions observed in the case of a pure PVA. The first corresponding to the PVA glass transition (at about 40°C)[43] and the second corresponding to the comelting of PVA and starch.

It seems like that the melting peak on the DSC curve before degradation was wider than that after degradation, and that is because the melting point was affected by both of the starch and PVA before degradation. We can see that the melting point was 223°C, which was between that of the pure corn starch (160°C) and PVA (230°C). After 1 day's degradation in SSF, the starch was decomposed quickly by the α-amylase. The residual ingredient was mainly PVA. So the width of the melting peak became narrower compared with that before degradation. From 8 to 30 day, due to the further degradation of starch, the melting point went up to 230°C, which is as same as the melting point of pure PVA. This phenomenon gave evidence that the starch has been already decomposed after 30 day's degradation, and this result was well consistent with that obtained from the weight loss test.

In SBF, the melting point maintained at 223°C from 1 to 8 days, which is longer than that in SSF (1 to 3 days). This phenomenon also demonstrates the degradation speed in SBF was smaller than that in SSF, and it was also consistent with that gotten from weight loss and SEM test.

The ΔH values were listed in Table VI. No matter in SBF or in SSF, the ΔH decreased as the degradation time increased (see Fig. 6). The decrease of the ΔH demonstrated the decrease of the crystallinity. The decrease of the crystallinity should be explained by that the degradation liquid dissolved into the small crystalline regions of the material. So part of the hydrogen bonds between the PVA or Starch molecules were replaced by those between the polymer and the water. The decrease of interaction force among the macromolecules resulted in the swelling, and the crystalline regions were gradually destroyed in the process of degradation and swelling. It was

TABLE VI
Changing of the Melting Enthalpy (Δ*H*) During Degradation

Samples	Δ*H* (J/g)			
	0d	1d	8d	30d
SBF	−186.3	−58.2	−60.4	−23.9
SSF	−186.3	−85.1	−77.2	−72.2

reported that the PVA melting enthalpy value decreased by decreasing the content of the starch in the case of uncross-linked starch/PVA.[43] In this work, it was found that the ΔH decreased in the process of degradation. It can also be explained by that the starch concentration decreased.

The *in vitro* biocompatibility evaluation

Cytotoxicity testing

Apart from favorable biodegradable and mechanical properties, the most important requirement for a biodegradable polymer to be applied in medical applications is its biocompatibility in a specific environment. Cytotoxicity testing represents the initial step in testing biocompatibility of potential biomaterials and medical devices.

Cytotoxicity ratios and the relative growth rate (RGR) of the tested biomaterial were calculated from the average OD values [see eq. (4)], and classified according to the following criteria for cytotoxicity: If RGR >100%, the corresponding cytotoxicity type was class 0, indicating no toxicity. If RGR = 0%, the corresponding cytotoxicity type was class 5, indicating the highest toxicity. 75–99%, 50–74%, 24–49%, and 1–25% RGR were categorized as class 1, 2, 3, and 4, respectively.

$$\mathrm{RGR} = \frac{\text{OD value of specimen suspension}}{\text{OD value of negative control suspension}} \times 100\%. \quad (4)$$

For all of the samples, the RGR was larger than 100% after 2 and 4 day's incubation, the cytotoxicity could be categorized as class 0 (See Fig. 7). It seems like that the SP films should accelerate the cells' growth. Maybe that can be attributed to the increase of the starch degradation products such as maltose, which can provide nutrientsubstance in the process of starch degradation. After 7 day's incubation, the RGR exhibited a slight decrease. This phenomenon was agreed with the regular rules that the cytotoxicity increased as the time increased. That was because the step by step release of the toxic substance. However, the RGR of all samples exceeded 90% (see Fig. 7), which demonstrates that the SP films have the excellent cell biocompatibility.

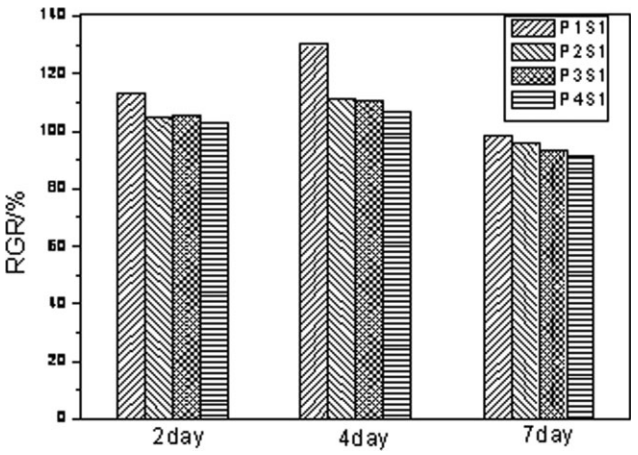

Figure 7 The Relative Growth Rates RGR (%) of the SP films.

Another obvious phenomenon is that the RGR increased as the starch content increased, and it can be observed at the same observation interval. This

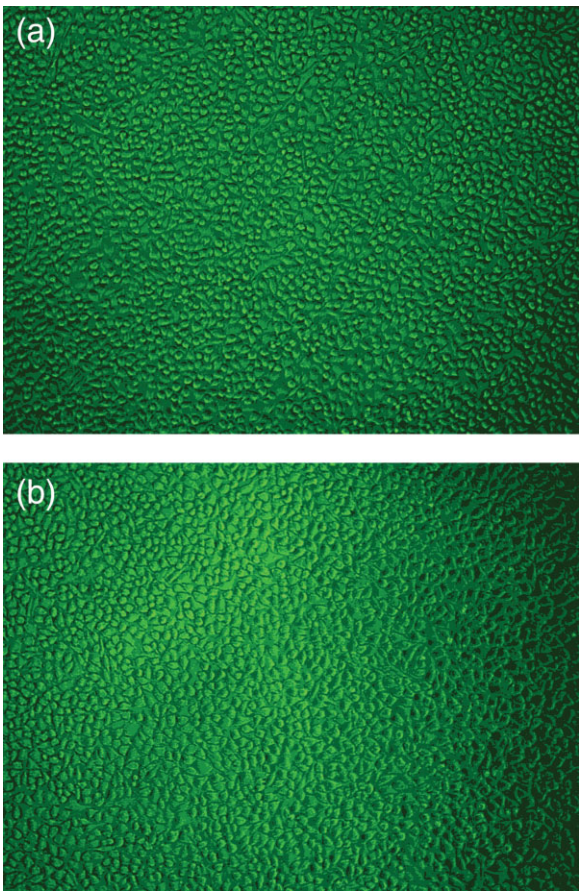

Figure 8 Morphology of the L929 cells after exposure to extract dilutions of P4S1 for 7 d: (a) negative control, (b) P4S1 extract dilution. [Color figure can be viewed in the online issue, which is available at www.interscience.wiley.com.]

phenomenon illustrated that the cell biocompatibility of starch was better than that of PVA.

Figure 8 reflects the cells' state after 7d in contact with the extraction of the P4S1. Cells in the extract dilution exhibited excellent state. The cells' dimension, shape, density, and refraction in the extracted liquid of P4S1 were very similar to those in negative control. It demonstrates the non toxicity of the SP films. The morphology of L929 cells in other samples' extract dilutions was similar to those in P4S1's extract dilutions.

L929 fibroblast attachment

The number and the shape of the cells which attached on surface of the membrane can reflect the cell biocompatibility directly. From the result of cytotoxicity we got that the RGR increased as the starch content increased, so we only chose P4S1 for observation. The morphology of attached cells on surface of P4S1 was observed.

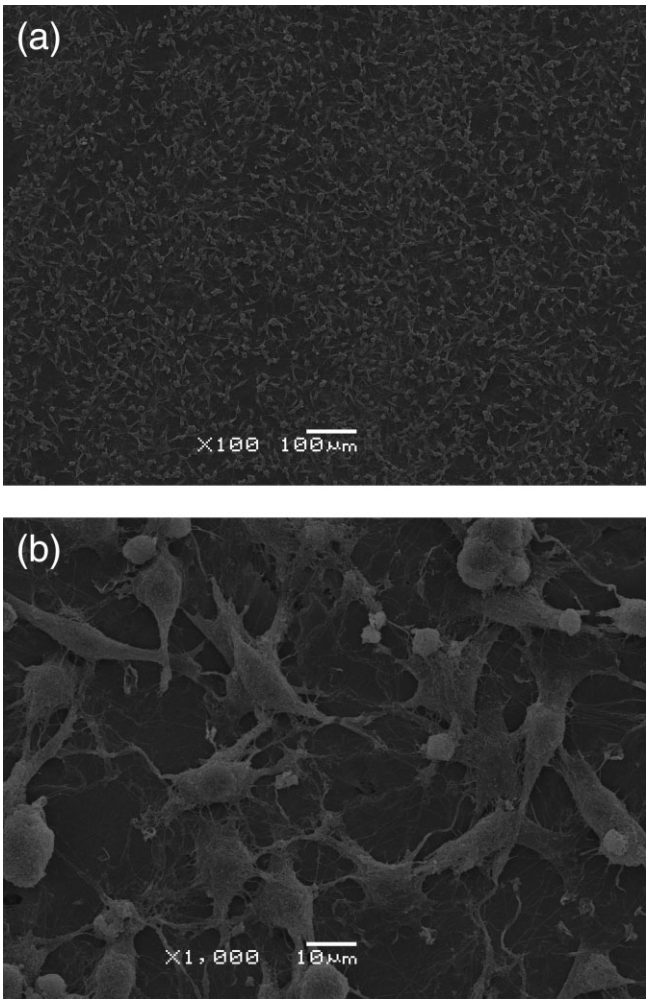

Figure 9 L929 fibroblast attachment on SP membranes (serum-containing, 72 h): (a) magnification × 100; (b) magnification × 1000.

TABLE VII
Hemolysis of Blood by Samples with Different Starch/PVA Ratio

Samples	Optical density at 545 nm	Hemolysis/%
Water	0.884	—
Saline	0.001	—
P4S1	0.023	2.49
P3S1	0.031	3.08
P2S1	0.020	2.15
P1S1	0.022	2.38

Figure 9 shows the results obtained from cell attachment experiments in serum-containing media conducted with P4S1 membrane. From Figure 9(a), we can see that there was a high cell density attached on surface of the film. From Figure 9(b) with the 1000 magnification, we can see a considerable amount of cells on the SP membrane spread and showed a flat, fibroblast morphology with their elongated shapes.

The results of the cells' morphology demonstrated the excellent cell affinity of the SP films.

Hemolysis analysis

Hemolysis of the blood is the problem associated with bio-incompatibility.[44] Red blood cells hemolysis when come in contact with water. This problem may be aggravated in the presence of an implant material. Results obtained for hemolysis of Wistar rats' blood with SP films were shown in Table VII. It was observed that the hemolysis ratios of all samples were less than 5%, which comes well within permissible limit.[45] The differences in hemolysis among the films with different starch/PVA ratio were not obvious. It may be conclude from the good blood compatibility that the SP films may be suitable as biomaterials for specific implant clinical application purpose.

CONCLUSIONS

The CA increased quickly with the time increased as a result of swelling. It took 10–20 min for different samples to reach to their maximum water absorption, and about 30 min to level off. The SD of the same sample dipping in SBF was larger than that in SSF.

Degradation in SSF was faster than that in SBF. In SSF, the weight loss of all samples exceeded the total weight percentage of starch and glycerol in the first day, and then it decreased slightly from 1 to 30 days. In SBF, the weight also lost quickly in the first day, but exhibited a step by step manner after that. PVA degraded very slowly under the normal body temperature both in SSF and SBF. The strength

and flexibility of the SP films in wet state could satisfy with the requirement of GTR membrane. No matter in SBF or SSF, although a rapid decrease happened in the first day, the mechanical properties decreased slightly after that. Results from the SEM showed that the films could keep their integrity even when the starch content reached 50 wt % and buried in SSF for 30 days. The improvement of the mechanical properties and integrity maintainability can be achieved by increasing the PVA content. The adjustable mechanical properties and excellent mechanical and integrity maintainability of the SP films are benefiting for their application as GTR membrane. DSC measurement showed that the coeffect melting peak was shifted and the width of the decreased during degradation. The changes were attributing to the degradation of the starch.

Besides, the SP films also showed excellent cell affinity with L929 fibroblasts and had the low hemolysis ratio. The *in vivo* biocompatibility of the SP films is under investigated.

References

1. Ozmeric, N.; Bal, B.; Oygur, T.; Balos, K. Periodontal Clin Invest 2000, 22, 22.
2. Fujihara, K.; Kotaki, M.; Ramakrishna, S. Biomaterials 2005, 26, 4139.
3. Hong, H.; Wei, J.; Liu, C. S. Composites: Part B 2007, 38, 311.
4. Liao, S.; Watari, F.; Zhu, Y. H.; Uo, M.; Akasaka, T.; Wang, W.; Xu, G. F.; Cui, F. Z. Dent Mater 2007, 23, 1120.
5. Beloti, M. M.; De Oliveira, P. T.; Gimenes, R.; Zaghete, M. A.; Bertolini, M. J.; Rosa, A. L. J Biomed Mater Res A 2006, 79, 282.
6. Mei, F.; Zhong, J. S.; Yang, X. P.; Ou Yang, X. Y.; Zhang, S.; Hu, X. Y.; Ma, Q.; Lu, J. G.; Seungkon, R. Biomacromolecules 2007, 8, 3729.
7. Piattelli, A.; Scarano, A.; Russo, P.; Matarasso, S. Biomaterials 1996, 17, 791.
8. Hammerle, C. H. F.; Schmid, J.; Lang, N. P.; Olah, A. J. J Oral Max Surg 1995, 53, 167.
9. Marouf, H. A.; El-Guindi, H. M. Oral Surg Oral Med Oral Pathol Oral Radiol Endod 2000, 89, 164.
10. Schmitz, J. P.; Lemke, R. R.; Zardeneta, G.; Hollinger, J. O. J Oral Maxillofac Surg 2000, 58, 888.
11. Rüdiger, S. G.; Ehmke, B.; Hommens, A.; Karch, H.; Flemmig, T. F. J Clin Periodontol 2003, 30, 19.
12. Ehmke, B.; Rudiger, S. G.; Hommens, A.; Karch, H.; Flemmig, T. F. J Clin Periodontol 2003, 30, 368.
13. Pretzl, B.; Kim, T. S.; Steinbrenner, H.; Dörfer, C.; Himmer, K.; Eickholz, P. J Clin Perio 2009, 36, 349.
14. Ishaug, S. L.; Crane, G. M.; Miller, M. J. J Biomed Mater Res 1997, 37, 17.
15. Ochi, K.; Chen, G. P.; Ushida, T.; Gojo, S.; Segawa, K.; Tai, H.; Ueno, K.; Ohkawa, H.; Mori, T.; Yamaguchi, A.; Toyama, Y.; Hata, J. I.; Umezawa, A. J Cell Physiol 2003, 194, 45.
16. Ma, P. X. Materialstoday 2004, 7, 30.
17. Mendes, S. C.; Reis, R. L.; Bovell, Y. P.; Cunha, A. M.; Van-Blitterswijk, C. A.; De-Bruijn, J. D. Biomaterials 2001, 22, 2057.
18. Gomes, M. E.; Sikavitsas, V. I.; Behravesh, E.; Reis, R. L.; Mikos, A. G. J Biomed Mater Res Part A 2003, 67, 87.
19. Salgado, A. J.; Coutinho, O. P.; Reis, R. L. Tissue Engin 2004, 10, 465.
20. Santos, M. I.; Fuchs, S.; Gomes, M. E.; Unger, R. E.; Reis, R. L.; Kirkpatrick, C. J. Biomaterials 2007, 28, 240.
21. Martins, A.; Chung, S.; Pedro, A. J.; Sousa, R. A.; Marques , A. P.; Reis, R. L.; Neves, N. M. J Tissue Eng Regen Med 2009, 3, 37.
22. Nakayama, Y.; Takatsuka, M.; Matsuda, T. Langmuir 1999, 15, 1667.
23. Hyon, S. H.; Cha, W. I.; Ikada, Y.; Kita, M.; Ogura, Y.; Honda, Y. J Biomater Sci, Polym Edn 1994, 5, 397.
24. Jiang, H. J.; Campbell, G.; Boughner, D.; Wan, W. K.; Quantz, M. Med Eng Phys 2004, 26, 269.
25. Wan, W. K.; Campbell, G.; Zhang, Z. F.; Hui, A. J.; Boughner, D. R. J Biomed Mater Res 2002, 63, 854.
26. Orloff, L. A.; Domb, A. J.; Teomim, D.; Fishbein, I.; Golomb, G. Adv Drug Deliver Rev 1997, 24, 3.
27. Yang, J. M.; Wen, Y. S.; Leu, T. L.; Yang, M. C. J Membr Sci 2004, 236, 39.
28. Pan, Y. S.; Xiong, D. S.; Ma, R. Y. Wear 2007, 262, 7.
29. Pan, Y. S.; Xiong, D. S. Wear 2009, 266, 699.
30. Young, T. H.; Chuang, W. Y.; Hsieh, M. Y.; Chen, L. W.; Hsu, J. P. Biomaterials 2002, 23, 3495.
31. Zhao, G. H.; Liu, Y.; Fang, C. L.; Zhang, M.; Zhou, C. Q.; Chen, Z. D. Polym Degrad Stabil 2006, 91, 703.
32. Chiellini, E.; Cinelli, P.; Chiellini, F.; Imam, S. H. Macromol Biosci 2004, 4, 218.
33. Chiellini, E.; Corti, A.; D'Antone, S.; Solaro, R. Prog Polym Sci 2003, 28, 963.
34. Caffesse, R. G.; Smith, B. A.; Castelli, W. A.; Nasjleti, C. E. J Periodontol 1988, 59, 589.
35. Iglhaut, J.; Aukhil, I.; Simpson, D. M.; Johnston, M. C.; Koch, G. J Periodontal Res 1998, 23, 107.
36. Liu, X.; Ding, C.; Wang, Z. Biomaterials 2001, 22, 2007.
37. Amaechi, B. T.; Higham, S. M. J Dent 2001, 29, 372.
38. Qi, M.; Wang, Q.; Ruan, M. S.; Wei, J.; Li, j; Jia, W. J Stomatol 2002, 22, 67.
39. Shi, R.; Liu, Q. Y.; Ding, T.; Han, Y. M.; Zhang, L. Q.; Chen, D. F.; Tian, W. J Appl Polym Sci 2007, 103, 574.
40. Shi, R.; Ding, T.; Liu, Q. Y.; Han, Y. M.; Zhang, L. Q.; Chen, D. F.; Tian, W. Polym Degrad Stabil 2006, 91, 3289.
41. Ueyama, Y.; Ishikawa, K.; Mano, T.; Koyama, T.; Nagatsuka, H.; Suzuki, K.; Ryoke, K. Biomaterials 2002, 23, 2027.
42. Zhu, Z. F. Carbohyd Polym 2003, 54, 115.
43. Cascone, M. G.; Barbani, N.; Cristallini, C.; Giusti, P.; Ciardelli, G.; Lazzeri, L. J Biomater Sci Polym Edn 2001, 12, 267.
44. Shim, D.; Wechsler, D. S.; Lloyd, T. R.; Beekman, R. H. Catheter Cardio Inter 1996, 39, 287.
45. Autian, J. Polymer Science and Technology, Kronenthal, R. L., Oser, Z., Martin, E., Eds. Plenum: New York, 1975; Chapter 8, p 181.